Geochemical Perspectives Letters

Core-mantle chemical interaction *via* convection within thermochemical piles

J. Korenaga[1*], S. Marchi[2]

OPEN ACCESS

https://doi.org/10.7185/geochemlet.2439

Abstract

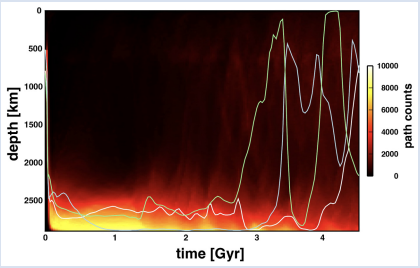

Dense thermochemical piles, widely believed to manifest themselves as large low-velocity shear provinces observed above the core-mantle boundary, are gravitationally stable against the ambient mantle, but convection can still happen within the piles. This "inter-pile convection" has two competing effects on core-mantle chemical interaction: one is to reduce the residence time of mantle material at the core-mantle boundary, and the other is to enhance the transfer of core-affected material. Based on convection diagnostics from the numerical simulations of thermochemical piles, we discuss how to constrain the likely formation mechanism of thermochemical piles using mantle geochemistry.

Received 16 July 2024 | Accepted 20 September 2024 | Published 10 October 2024

Introduction

The silicate mantle and the metallic core interact both thermally and chemically at the core-mantle boundary (CMB). Thermal interaction manifests as core heat flux, which has long been studied by numerous authors because of its importance for plume dynamics (*e.g.*, Sleep, 1990), the geodynamo (*e.g.*, Nimmo, 2015), and Earth's thermal evolution (*e.g.*, Korenaga, 2008). By contrast, less attention has traditionally been paid to chemical interactions, largely because chemical diffusion can be slower than thermal diffusion by many orders of magnitude and other possible transfer mechanisms are not well understood (*e.g.*, Porcelli and Halliday, 2001; Walker and Walker, 2005). However, recent years have witnessed a growing number of observational, experimental, and theoretical studies that consider the possibility of core-mantle chemical interaction to explain the geochemistry of ocean island basalts (OIBs) (*e.g.*, Mundl *et al.*, 2017; Rizo *et al.*, 2019; Yoshino *et al.*, 2020; Olson and Sharp, 2022; Ferrick and Korenaga, 2023b; Deng and Du, 2023; Horton *et al.*, 2023). For example, negative μ^{182}W anomalies reported for OIB (*e.g.*, Mundl *et al.*, 2017), especially in conjunction with their negative correlation with ^{3}He/^{4}He, are difficult to explain without some interactions with the core, which is considered to have a strongly negative μ^{182}W value.

The CMB region is physically and chemically heterogeneous, as indicated by the presence of large low shear-velocity provinces (LLSVPs) and ultra-low velocity zones (ULVZs) (*e.g.*, Garnero *et al.*, 2016). The LLSVPs appear to be the source regions for most large igneous provinces (Burke and Torsvik, 2004), which in turn often serve as the precursors of hot spot magmatism (Richards *et al.*, 1989). Thus, the nature of core-mantle chemical interaction at the LLSVPs becomes important when considering how possible core signatures can be imparted to the OIB source mantle. Based on their apparent longevity (Torsvik *et al.*, 2014), the LLSVPs have been suggested to represent thermochemical piles compositionally denser than the ambient mantle. Whereas this presumed intrinsic density anomaly can stabilise thermochemical piles against the ambient mantle, convection can still take place within the piles themselves. The purpose of this paper is to investigate the potential role of this convection within a thermochemical pile, or "inter-pile convection", in core-mantle chemical interaction. ULVZs may contribute to the geochemistry of the OIB source mantle, but given their global distribution and highly variable characteristics (*e.g.*, Hansen *et al.*, 2023), their role in hot spot magmatism is not very clear, and it is beyond the scope of this paper. Core-mantle interaction affects both the ambient mantle and thermochemical piles, but core signatures imparted to the former would be quickly diluted by convective mixing with the bulk mantle. By contrast, dense piles could potentially reside on the CMB for billions of years and acquire strong core signatures, and despite its limited surface coverage on the CMB (~30 %), they could play a disproportionate role in creating chemical heterogeneities in the mantle. Because of inter-pile convection, however, their longevity does not necessarily translate to strong core signals in the geochemistry of OIB source mantle.

Inter-pile convection has two competing effects. Without it, core-mantle chemical interactions would affect only the lowermost portion of the piles, most of which would remain inaccessible. With convection, the base of the piles can be brought directly to the top of the piles, facilitating sampling by mantle plumes. At the same time, convective mixing within piles dilutes the effect of core-mantle chemical interactions. Imparting core signatures on the OIB source mantle, therefore, depends on

1. Department of Earth and Planetary Sciences, Yale University, P.O. Box 208109, New Haven, CT 06520, USA
2. Department of Space Studies, Southwest Research Institute, 1301 Walnut Street, Boulder, CO 80302, USA
* Corresponding author (email: jun.korenaga@yale.edu)

how directly inter-pile convection can bring materials from the bottom to the top and side boundaries, where mixing with the ambient mantle allows the entrainment of dense pile materials. Quantifying the efficiency of such convective transfer is, however, not straightforward because the volume of thermochemical piles can be time dependent; they could have been smaller if they represent accumulated subducted materials (*e.g.*, Christensen and Hofmann, 1994) or larger if they are primordial anomalies (*e.g.*, Korenaga and Marchi, 2023). This fundamentally transient nature of inter-pile convection makes it difficult to build a generic model. In this study, therefore, we opt to present a case study by utilising our earlier numerical model of thermochemical piles (Korenaga and Marchi, 2023). Even though this model is based on a particular hypothesis for pile formation, our approach of characterising the nature of inter-pile convection is sufficiently general, allowing us to discuss core-mantle chemical interaction in the presence of inter-pile convection.

Convection Diagnostics with Dense Tracers

Our convection model was designed to study the fate of a metal-impregnated layer formed in the mid-mantle resulting from a large late accretion impact (Korenaga and Marchi, 2023) (Fig. 1a). The metal-impregnated layer contains $\sim 1 \times 10^{22}$ kg of metal (corresponding to ~1–2 % density anomalies), and it first sinks to the CMB by the Rayleigh-Taylor instability (Fig. 1b). The layer is then gradually entrained by mantle convection, increasing the abundance of highly siderophile elements (HSE) in the ambient mantle (Fig. 1c–f). Our hypothesis is that the LLSVPs represent the residue of this metal-impregnated layer. The details of our convection modelling are given in the Supplementary Information. Even though this convection model was originally built to test the feasibility of our hypothesis, our modelling results can also be utilised to discuss inter-pile convection in a more general context.

The fate of the metal-impregnated layer is tracked by dense tracers that represent metallic components, and their trajectories contain valuable information on the nature of inter-pile convection (Fig. 1g). As the metal-impregnated layer initially descends to the CMB, most of dense tracers become part of thermochemical piles, and they circulate within the piles before being entrained by the ambient mantle. We focus on the dense tracers that initially sank to the bottom 10 % of the mantle and monitor their trajectories up to the time of their entrainment, t_e (defined as the time when a tracer enters the upper half of the mantle). The criterion of the bottom 10 % is chosen to easily identify dense particles that constitute long lived piles. For each trajectory, we measure the number of extrema (N_x) of its vertical coordinate as well as the minimum distance to the CMB. The transit time scale, τ_T, or the average period of particle motion within convection, is estimated as $2t_e/(N_x)$ (Fig. 2a).

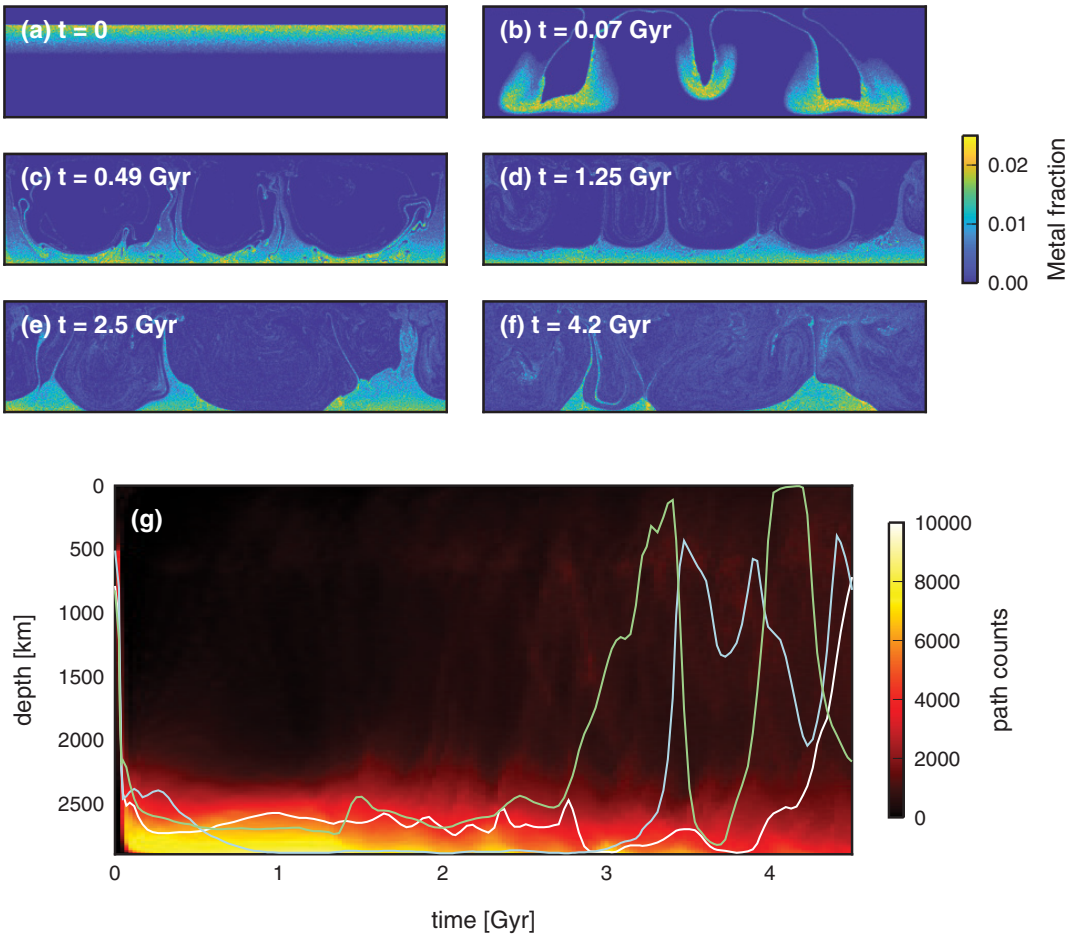

Figure 1 **(a–f)** Snapshots of the composition field for the case starting with a laterally homogeneous, 750 km thick metal-impregnated layer with the total metal of 10^{22} kg, and with $Ra = 3 \times 10^7$, non-dimensional internal heating of 25, and the Frank-Kamenetskii parameter $\theta = 4.61$. See Figure S-1 for the corresponding temperature field. **(g)** Summary of vertical trajectories of dense tracers, with three sample trajectories highlighted.

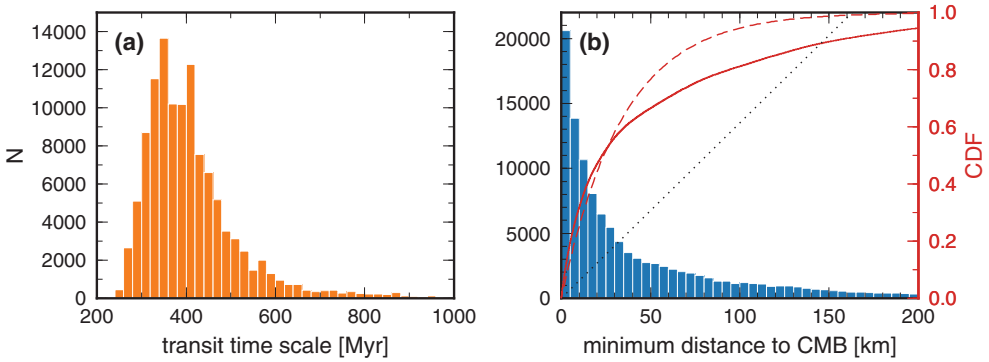

Figure 2 Histograms of **(a)** transit time scale and **(b)** minimum distance to CMB, measured from the trajectories of dense tracers for the case shown in Figure 1. Also shown in **(b)** are the corresponding cumulative distribution function (CDF) in red, a fitted exponential CDF in red-dashed, and a reference uniform CDF in dotted.

To quantify how directly inter-pile convection can bring core signatures to its boundaries, we need to know the fate of mantle parcels that directly touch the CMB, and our inference is based on the statistics of the minimum distance to the CMB for dense tracers (Fig. 2b). The distribution of the minimum distance is usually similar to the exponential distribution. In thermal convection, the delamination of the bottom boundary layer is the source of upwelling, and simply bringing the bottom boundary layer to the top of the pile would result in a relatively uniform distribution of the minimum distance, within the length scale corresponding to the thickness of the boundary layer. We define the amplification factor as a measure of deviations from this expected uniform distribution (see the Supplementary Information for details). The amplification factor of three, for example, means that entraining the mantle parcels that have directly touched the CMB is three times more likely than expected from the simple upwelling of a bottom boundary layer.

As expected, the transit time scale is basically a function of the Rayleigh number (Fig. 3a), and a higher Rayleigh number (*i.e.* lower viscosity) results in a shorter transit time scale. The transit time scale does not vary much as a function of the entrainment ratio, which measures the fraction of entrained tracers among the dense tracers that initially sank to the bottom 10 % of the mantle. The statistics of the amplification factor are more variable (Fig. 3b). Considerable scatters are seen at low entrainment ratios because of the overpopulation of dense tracers in the piles. In these cases, dense tracers located near the CMB are unlikely to ever be entrained, and thus the distribution of the minimum distance for the entrained tracers does not necessarily take its maximum at zero distance. For relatively high entrainment ratios (>0.5), the amplification factor is consistently ~3 to ~4.

Discussion: Origins of Thermochemical Piles

The characterisation of inter-pile convection allows us to evaluate the strengths and the weaknesses of the existing hypotheses put forward for the origin of thermochemical piles. The diagnostics of inter-pile convection given in the previous section are based on one scenario for pile formation, but the main points of our discussion should remain valid as long as inter-pile convection is concerned. Here we focus on whether a given hypothesis can explain the correlation between the He and W isotopes observed in OIBs (Mundl *et al.*, 2017; Mundl-Petermeier *et al.*, 2020). A recent modelling study suggests that both He and W isotope signatures can be explained by core-mantle chemical interaction (Ferrick and Korenaga, 2023b), but this model treats the OIB source mantle (or equivalently, thermochemical piles) as a static reservoir lying on the CMB. Based on experiments on W diffusivity through lower mantle minerals (Yoshino *et al.*, 2020), the W isotopic signature of the core can diffuse into the bottom ~20 km of the mantle over four billion years, but this time scale for chemical interaction is much longer than the transit time scale (Fig. 3a), which is a more appropriate diffusion time scale in the presence of inter-pile convection. With a residence time of only 200 Myr, for example, the diffusion length would be

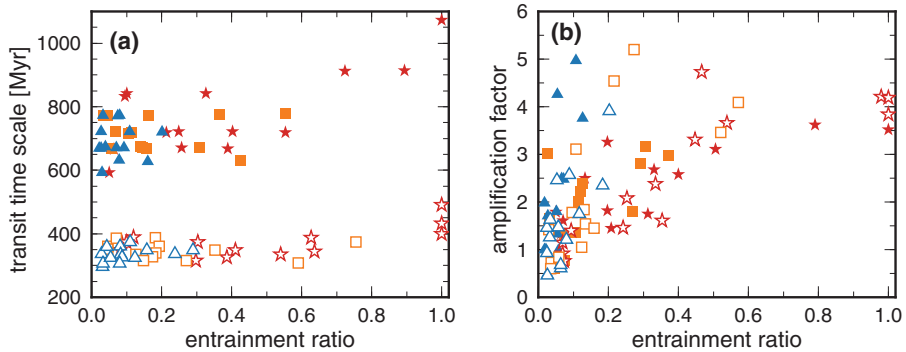

Figure 3 Summary of convection diagnostics for all model runs: **(a)** transit time scale and **(b)** amplification factor. Solid and open symbols for $Ra = 10^7$ and 3×10^7, respectively, and stars, squares, and triangles denote the cases with the Frank-Kamenetskii parameter θ of 4.61, 5.70, and 6.91, respectively.

reduced to ~4.5 km. At the same time, inter-pile convection can efficiently deliver this thin core-affected layer to the OIB source mantle, so it is still possible to reproduce the observed isotope correlation by core-mantle interaction. In this case, scatters in the observed correlation are likely caused by the stochastic nature of convective mass transfer, instead of differences in the sampled depth as originally proposed (Ferrick and Korenaga, 2023b).

Inter-pile convection can transport core signatures over a few hundred kilometres, but whether such mass transfer would be quantitatively sufficient still depends on the efficiency of diffusive interaction across the CMB. Consider, for example, the Hawaiian plume, which is the most volumetrically significant plume with its plume buoyancy flux estimated to be $\sim 5 \times 10^3$ kg s^{-1} (Sleep, 1990; King and Adam, 2014). By dividing the buoyancy flux with the product of thermal expansivity (3×10^{-5} K^{-1}) and a temperature contrast (200 K), we obtain the corresponding mass flux of $\sim 8 \times 10^5$ kg s^{-1}. If the average μ^{182}W anomaly of Hawaiian basalts is −5 (Willhite *et al.*, 2024) and the core μ^{182}W anomaly is −220, ~2.3 % of the source mantle must diffusively interact with the core. To provide such a source mantle for the duration of 20 Myr, for example, the mass of core-affected material needs to be $\sim 10^{11}$ kg. This translates to the thickness of core-affected layer of ~670 m, with the density of the lowermost mantle (5500 kg m^{-3}) and the radius of the plume stem area of 500 km. For the residence time along the CMB of 200 Myr, this diffusion length scale requires W diffusivity to be greater than 1.7×10^{-11} m^2 s^{-1}. Higher W diffusivities have been suggested for the CMB conditions ($\sim 8 \times 10^{-8}$ m^2 s^{-1}) (Yoshino *et al.*, 2020), but this involves considerable extrapolations from the experimental conditions of 1600–1900 K and 25 GPa to the CMB conditions of ~4000 K and 130 GPa. Thus, if the actual W diffusivity at the CMB conditions were too low, core-mantle interaction would be insufficient to explain the observed W isotopic signatures. The same consideration applies to the He isotopic signatures, but the situation is different from imparting core W isotopic signatures, which involves only isotope exchange across the CMB with no net W flux. On the other hand, the transfer of core He isotopic signatures depends on the net diffusional flux of He across the CMB, which is proportional not only to the He diffusivity but also to the He concentration in the core, both of which are poorly constrained (Olson and Sharp, 2022).

Thus, W diffusivity at the CMB conditions, along with the transit time scale of inter-pile convection, may be the key to distinguishing different formation hypotheses for thermochemical piles. If the W diffusivity is too low to explain the magnitude of hot spot magmatism with W isotope anomalies, pile formation mechanisms without involving metallic components (*e.g.*, Christensen and Hofmann, 1994; Yuan *et al.*, 2023) would be difficult to explain the observed W isotope signatures. By contrast, W diffusivity becomes irrelevant for pile formation by late accretion (Korenaga and Marchi, 2023) because the core-like W isotope signatures (μ^{182}W of −220) are already embedded in the piles from the outset. Note that, contrary to our earlier conjecture (Korenaga and Marchi, 2023), pile formation by late accretion can still satisfy the observed absence of correlation between μ^{182}W and HSE concentrations (Mundl *et al.*, 2017). To be entrained and become part of the OIB source mantle, the density anomaly of pile materials must be compensated by the thermal buoyancy of hot ambient mantle, and as a result, pile materials can constitute only ~10 % of the OIB source mantle (Ferrick and Korenaga, 2023b). Mixing with the ambient mantle during entrainment thus sufficiently dilutes the effect of metallic components. A major challenge for the late accretion-based hypothesis is instead how to explain the correlation between He and W isotope anomalies. Because W isotope signatures would be sufficiently strong everywhere within the piles, the magnitude of He isotope signatures need to be similarly ubiquitous, requiring efficient ^{3}He transport from the core to the mantle. The slopes of the correlations between μ^{182}W and ^{3}He/^{4}He vary from plume to plume (or even within a single plume), and some plume-derived systems (*e.g.*, Baffin Bay) are characterised by very high ^{3}He/^{4}He but no W anomaly (*e.g.*, Mundl-Petermeier *et al.*, 2020; Willhite *et al.*, 2024). It is to be seen whether such complexity of observations can be explained by the combination of core-mantle interaction and inter-pile convection.

The threshold diffusivity for W is suggested to be on the order of 10^{-11} m^2 s^{-1} in the above, but there are a few important assumptions, the validity of which requires more careful analyses of hot spot magmatism. First, we need to accurately estimate the spatial and temporal average of a W isotope anomaly for a given mantle plume. If very negative μ^{182}W signatures are spatially or temporally localised features, the required volume of core-affected materials could be substantially reduced. Second, plume buoyancy fluxes themselves are subject to non-trivial uncertainties (*e.g.*, King and Adam, 2014). It is also important to consider various types of diffusive interactions. For example, the present day core-side temperature of the CMB is close to the mantle solidus, so the lowermost part of the mantle is likely to have been partially molten when the core was hotter in the past. This tendency is even more important for the piles because they are generally hotter than the ambient mantle. Diffusive transport of core signatures would be rapid through a partially molten mantle. Though it seems difficult to maintain a partially molten state as melt is denser than the coexisting solid phase at the CMB conditions (*e.g.*, Nomura *et al.*, 2011) and likely drains downward, it may be possible to avoid downward percolation by convective stirring (Hernlund and Jellinek, 2010).

Direct mass transfer from the core can also be treated as a diffusive process by defining an 'effective' diffusion coefficient. Whereas the penetration of molten iron into the lower mantle by morphological instability may be unlikely (Yoshino, 2019), MgO exsolution from a cooling core can still happen if the core was initially saturated with Mg (Deng and Du, 2023). This mechanism is important for our discussion because efficient exsolution could result in a high effective W diffusivity, but its efficacy is still uncertain. One important point is that a substantial fraction of an impactor's core would directly merge with the target's core (Marchi *et al.*, 2018), *i.e.* without chemically equilibrating with the target's mantle. Thus, the early core is not necessarily saturated with Mg, and the weak temperature dependence of Mg solubility in the core (Du *et al.*, 2019) further reduces the likelihood of MgO exsolution. MgO exsolution was originally proposed to explain the early geodynamo (O'Rourke and Stevenson, 2016), but it is also possible to explain the early geodynamo without invoking MgO exsolution (Ferrick and Korenaga, 2023a).

Delineating the origin of thermochemical piles using mantle geochemistry will thus require further observational, experimental, and theoretical efforts. It is hoped that our exploration of inter-pile convection will serve as a useful theoretical reference when assimilating the outcomes of future research.

Acknowledgements

This research was supported in part by the U.S. National Science Foundation EAR-2102777 and EAR-2102571. The authors thank Richard Walker and an anonymous reviewer for their constructive comments.

Editor: Anat Shahar

Additional Information

Supplementary Information accompanies this letter at https://www.geochemicalperspectivesletters.org/article2439.

Cite this letter as: Korenaga, J., Marchi, S. (2024) Core-mantle chemical interaction *via* convection within thermochemical piles. *Geochem. Persp. Let.* 32, 34–38. https://doi.org/10.7185/geochemlet.2439

References

Burke, K., Torsvik, T.H. (2004) Derivation of Large Igneous Provinces of the past 200 million years from long-term heterogeneities in the deep mantle. *Earth and Planetary Science Letters* 227, 531–538. https://doi.org/10.1016/j.epsl.2004.09.015

Christensen, U.R., Hofmann, A.W. (1994) Segregation of subducted oceanic crust in the convecting mantle. *Journal of Geophysical Research: Solid Earth* 99, 19867–19884. https://doi.org/10.1029/93JB03403

Deng, J., Du, Z. (2023) Primordial helium extracted from the Earth's core through magnesium oxide exsolution. *Nature Geoscience* 16, 541–545. https://doi.org/10.1038/s41561-023-01182-7

Du, Z., Boujibar, A., Driscoll, P., Fei, Y. (2019) Experimental Constraints on an MgO Exsolution-Driven Geodynamo. *Geophysical Research Letters* 46, 7379–7385. https://doi.org/10.1029/2019GL083017

Ferrick, A.L., Korenaga, J. (2023a) Defining Earth's elusive thermal budget in the presence of a hidden reservoir. *Earth and Planetary Science Letters* 601, 117893. https://doi.org/10.1016/j.epsl.2022.117893

Ferrick, A.L., Korenaga, J. (2023b) Long-term core–mantle interaction explains W-He isotope heterogeneities. *Proceedings of the National Academy of Sciences* 120, e2215903120. https://doi.org/10.1073/pnas.2215903120

Garnero, E.J., McNamara, A.K., Shim, S.-H. (2016) Continent-sized anomalous zones with low seismic velocity at the base of Earth's mantle. *Nature Geoscience* 9, 481–489. https://doi.org/10.1038/ngeo2733

Hansen, S.E., Garnero, E.J., Li, M., Shim, S.-H., Rost, S. (2023) Globally distributed subducted materials along the Earth's core-mantle boundary: Implications for ultralow velocity zones. *Science Advances* 9, eadd4838. https://doi.org/10.1126/sciadv.add4838

Hernlund, J.W., Jellinek, A.M. (2010) Dynamics and structure of a stirred partially molten ultralow-velocity zone. *Earth and Planetary Science Letters* 296, 1–8. https://doi.org/10.1016/j.epsl.2010.04.027

Horton, F., Asimow, P.D., Farley, K.A., Curtice, J., Kurz, M.D., Blusztajn, J., Biasi, J.A., Boyes, X.M. (2023) Highest terrestrial $^{3}He/^{4}He$ credibly from the core. *Nature* 623, 90–94. https://doi.org/10.1038/s41586-023-06590-8

King, S.D., Adam, C. (2014) Hotspot swells revisited. *Physics of the Earth and Planetary Interiors* 235, 66–83. https://doi.org/10.1016/j.pepi.2014.07.006

Korenaga, J. (2008) Urey ratio and the structure and evolution of Earth's mantle. *Reviews of Geophysics* 46, RG2007. https://doi.org/10.1029/2007RG000241

Korenaga, J., Marchi, S. (2023) Vestiges of impact-driven three-phase mixing in the chemistry and structure of Earth's mantle. *Proceedings of the National Academy of Sciences* 120, e2309181120. https://doi.org/10.1073/pnas.2309181120

Marchi, S., Canup, R.M., Walker, R.J. (2018) Heterogeneous delivery of silicate and metal to the Earth by large planetesimals. *Nature Geoscience* 11, 77–81. https://doi.org/10.1038/s41561-017-0022-3

Mundl, A., Touboul, M., Jackson, M.G., Day, J.M.D., Kurz, M.D., Lekic, V., Helz, R.T., Walker, R.J. (2017) Tungsten-182 heterogeneity in modern ocean island basalts. *Science* 356, 66–69. https://doi.org/10.1126/science.aal4179

Mundl-Petermeier, A., Walker, R.J., Fischer, R.A., Lekic, V., Jackson, M.G., Kurz, M.D. (2020) Anomalous ^{182}W in high $^{3}He/^{4}He$ ocean island basalts: Fingerprints of Earth's core? *Geochimica et Cosmochimica Acta* 271, 194–211. https://doi.org/10.1016/j.gca.2019.12.020

Nimmo, F. (2015) 8.02 - Energetics of the Core. In: Schubert, G. (Ed.) *Treatise on Geophysics*. Second Edition, Elsevier, Amsterdam, 8, 27–55. https://doi.org/10.1016/B978-0-444-53802-4.00139-1

Nomura, R., Ozawa, H., Tateno, S., Hirose, K., Hernlund, J., Muto, S., Ishii, H., Hiraoka, N. (2011) Spin crossover and iron-rich silicate melt in the Earth's deep mantle. *Nature* 473, 199–202. https://doi.org/10.1038/nature09940

Olson, P.L., Sharp, Z.D. (2022) Primordial Helium-3 Exchange Between Earth's Core and Mantle. *Geochemistry, Geophysics, Geosystems* 23, e2021GC009985. https://doi.org/10.1029/2021GC009985

O'Rourke, J.G., Stevenson, D.J. (2016) Powering Earth's dynamo with magnetism precipitation from the core. *Nature* 529, 387–389. https://doi.org/10.1038/nature16495

Porcelli, D., Halliday, A.N. (2001) The core as a possible source of mantle helium. *Earth and Planetary Science Letters* 192, 45–56. https://doi.org/10.1016/S0012-821X(01)00418-6

Richards, M.A., Duncan, R.A., Courtillot, V.E. (1989) Flood Basalts and Hot-Spot Tracks: Plume Heads and Tails. *Science* 246, 103–107. https://doi.org/10.1126/science.246.4926.103

Rizo, H., Andrault, D., Bennett, N.R., Humayun, M., Brandon, A., Vlastelic, I., Moine, B., Poirier, A., Bouhifd, M.A., Murphy, D.T. (2019) ^{182}W evidence for core-mantle interaction in the source of mantle plumes. *Geochemical Perspectives Letters* 11, 6–11. https://doi.org/10.7185/geochemlet.1917

Sleep, N.H. (1990) Hotspots and mantle plumes: Some phenomenology. *Journal of Geophysical Research: Solid Earth* 95, 6715–6736. https://doi.org/10.1029/JB095iB05p06715

Torsvik, T.H., van der Voo, R., Doubrovine, P.V., Burke, K., Steinberger, B., Ashwal, L.D., Trønnes, R.G., Webb, S.J., Bull, A.L. (2014) Deep mantle structure as a reference frame for movements in and on the Earth. *Proceedings of the National Academy of Sciences* 111, 8735–8740. https://doi.org/10.1073/pnas.1318135111

Walker, R.J., Walker, D. (2005) Does the core leak? *EOS* 86, 237–242. https://doi.org/10.1029/2005EO250001

Willhite, L.N., Finlayson, V.A., Walker, R.J. (2024) Evolution of tungsten isotope systematics in the Mauna Kea volcano provides new constraints on anomalous $\mu^{182}W$ and high $^{3}He/^{4}He$ in the mantle. *Earth and Planetary Science Letters* 640, 118795. https://doi.org/10.1016/j.epsl.2024.118795

Yoshino, T. (2019) Penetration of molten iron alloy into the lower mantle phase. *Comptes Rendus Géoscience* 351, 171–181. https://doi.org/10.1016/j.crte.2018.06.013

Yoshino, T., Makino, Y., Suzuki, T., Hirata, T. (2020) Grain boundary diffusion of W in lower mantle phase with implications for isotopic heterogeneity in oceanic island basalts by core-mantle interactions. *Earth and Planetary Science Letters* 530, 115887. https://doi.org/10.1016/j.epsl.2019.115887

Yuan, Q., Li, M., Desch, S.J., Ko, B., Deng, H., Garnero, E.J., Gabriel, T.S.J., Kegerreis, J.A., Miyazaki, Y., Eke, V., Asimow, P.D. (2023) Moon-forming impactor as a source of Earth's basal mantle anomalies. *Nature* 623, 95–99. https://doi.org/10.1038/s41586-023-06589-1

Geochemical Perspectives Letters

Core-mantle chemical interaction *via* convection within thermochemical piles

J. Korenaga, S. Marchi

Supplementary Information

The Supplementary Information includes:

- Modeling Thermochemical Piles in Whole Mantle Convection
- Quantifying the Efficiency of Transporting Core Signatures
- Figures S-1 and S-2
- Supplementary Information References

Modeling Thermochemical Piles in Whole Mantle Convection

Governing equations and boundary conditions

The convection modeling reprocessed here is based on the nondimensionalized governing equations for thermal convection of an incompressible fluid, consisting of the conservation of mass, momentum, and energy (see Korenaga and Marchi, 2023, for these equations). The spatial coordinates are normalized by the mantle depth D (=2900 km), and time is normalized by the diffusion time scale, D^2/κ, where κ is thermal diffusivity (=10^{-6} m^2 s^{-1}). Temperature is normalized by a potential temperature difference between the surface and the core-mantle boundary, ΔT (=2000 K). The Rayleigh number Ra is defined here as:

$$Ra = \frac{\alpha \rho_0 g \Delta T D^3}{\kappa \eta_0},$$

where α is thermal expansivity (= 10^{-5} K^{-1}), ρ_0 is reference density (= 5000 kg m^{-3}), g is gravitational acceleration, and η_0 is the reference viscosity. Nondimensional heat generation is defined as:

$$H^* = \frac{\rho_0 H D^2}{k \Delta T},$$

where H is heat production rate per unit mass, and k is thermal conductivity. We tested a few values of H^* to achieve Earth-like internal heating rate (~0.6–0.7), which includes the effect of secular cooling (Korenaga, 2017). Viscosity is both temperature- and depth-dependent. The temperature dependence is prescribed by:

$$\eta_T^* = \exp[\theta(1 - T^*)],$$

where θ is called the Frank-Kamenetskii parameter, and the reference viscosity for the bottom three quarters of the mantle is raised by a factor of 30 (Hager, 1984).

The above governing equations are solved with the two-dimensional finite element code of Korenaga and Jordan (2003). The top and bottom boundaries are free slip. The top and bottom (nondimensional) temperatures are set to 0 and 1, respectively. A reflecting (*i.e.* free slip and insulating) boundary condition is applied to the side boundaries. The aspect ratio of a model is four to reduce wall effects, and the model is discretized by 400×100 uniform quadrilateral elements. Internal temperature is set to 0.7 at $t^* = 0$ with random perturbations of small amplitude (10^{-3}), and the system is integrated until $t^* = 0.0169$, which corresponds to 4.5 billion years.

Chemical tracers

The chemical composition is tracked by 10^8 tracers, which are initially randomly distributed and are advected with a fourth-order Runge-Kutta scheme (Christensen and Yuen, 1984). A certain fraction of these tracers are associated with a density anomaly of 4000 kg m^{-3} to represent metallic components. For a total metal mass of 10^{22} kg, for example, 0.25% of the tracers (2.5×10^5 tracers) are marked as dense tracers. Based on the results of three-phase flow modeling of Korenaga and Marchi (2023), such dense tracers are distributed at mid-mantle depths, corresponding to the location of a hypothetical partially molten zone. With a total metal mass of 10^{22} kg, a laterally homogeneous, 750-km thick partially molten zone would have an average metal concentration of ~0.97 wt%, and because metal concentration is expected to vary linearly within the zone, dense tracers are distributed so that the concentration is ~1.93 wt% at the top of the zone and linearly decreases to zero at its bottom. This would correspond to the case of a 3% Earth mass impactor with an impact angle of 45° and v/v_e=2.2 (Korenaga and Marchi, 2023; see their Table S3). We tested seven different initial tracer distributions. Four of them are with laterally homogeneous partially molten zones, all with the total metal mass of 10^{22} kg, the complete mixing of which would reproduce the present-day mantle abundance of HSEs. The thickness of the zone is 250 km (Case 1), 500 km (Case 2), 750 km (Case 3), and 1000 km (Case 4). The rest of the cases all have a 1000-km thick partially molten zone with a locally deep, 500-km thick partially molten zone for the mid-50% of the lateral extent. The total amount of metal in the deep zone is the same as that in the shallow zone in Case 5, and it is greater by 25% in Case 6 and 50% in Case 7. Thus, the total metal mass is 1.13×10^{22} kg in Case 6 and 1.25×10^{22} kg in Case 7.

Notes on modeling strategy

One of the important questions about the dynamics of thermochemical piles is how dense piles are entrained by the upwelling of the ambient mantle. The competition between thermal and chemical buoyancies near the core-mantle boundary region determines the efficiency of such convective entrainment, and this is the rationale behind the values adopted for thermal expansivity (10^{-5} K^{-1}) and reference density (5000 kg m^{-3}), both of which are appropriate for the lowermost mantle. We tested two Rayleigh numbers, 10^7 and 3×10^7, and with these material properties, they correspond to the reference viscosity of 2.4×10^{21} Pa s and 8×10^{20} Pa s, respectively.

For each of the two Rayleigh numbers, we have tested all of the seven initial tracer distributions, two internal heat production (20 and 25 for Ra=10^7, and 25 and 30 for Ra=3×10^7), and three Frank-Kamenetskii parameters (4.61, 5.70, and 6.91, which corresponds to the total viscosity contrast due to temperature of 10^2, 3×10^2, and 10^3, respectively), amounting to a total of 84 model runs. In general, greater temperature dependence of viscosity brings the system closer to stagnant lid convection, thereby decreasing the mixing efficiency as well as the surface heat flux (Korenaga and Marchi, 2023; see their Figure S3). For example, with the Frank-Kamenetskii parameter θ of 6.91, only ~20 to ~50% of the original thermochemical piles is eventually entrained, whereas with θ of 4.61, the entrainment efficiency is generally doubled.

We use the same temperature dependence of viscosity for both the upper mantle and lower mantle, and this may appear as a gross simplification. However, using a more complicated setting of mantle rheology does not necessarily yield more useful modeling results, because our primary goal is to understand the long-term dynamics of thermochemical piles. To simulate long-term convective interactions between the ambient mantle and thermochemical piles, it is important to maintain subduction and thus plate tectonics. If the mode of mantle convection is instead stagnant lid convection, convective currents in the mantle are characterized by small-scale thermal anomalies, which would reduce the efficiency of convective entrainment. We can avoid stagnant lid convection, either by using weak enough temperature-dependent viscosity or by using the combination of strongly temperature-dependent viscosity with some weakening mechanisms (*e.g.*, Bercovici *et al*., 2015), and we use the former for simplicity. The latter would be important if we are interested in simulating plate tectonics in more detail (*e.g.*, reproducing the high 'plateness'). The detailed rheology of the lower mantle is still largely unknown. From the studies of instantaneous Stokes flow and postglacial rebound, it is generally agreed that the lower mantle has a higher average viscosity (by a factor of 10 to 100) than the upper mantle (*e.g.*, Hager, 1984; Forte *et al*., 2015), but further details are subject to debate. Even the sign of the temperature dependence of viscosity is not settled yet, and the Frank-Kamenetskii parameter θ can be negative in the lower mantle (Solomatov, 1996, 2001; Korenaga, 2005; Frazer and Korenaga, 2022). We have varied the parameter θ from 4.61 to 6.91, to examine the sensitivity of our modeling results to the temperature dependence of viscosity, without implying which one would be most realistic. The cases with θ of 4.61 are generally most effective in entraining thermochemical piles, thus raising the mantle abundance of highly siderophile elements to a satisfactory level. This by itself does not mean that the actual temperature dependence of lower mantle viscosity is well represented by this value

of the Frank-Kamenetskii parameter. Nevertheless, this value of θ does correspond to a reasonable viscosity structure of the mantle. With the Rayleigh number of 3×10^7 or the reference viscosity of 8×10^{20} Pa s, the viscosity at the CMB (*i.e.* T^* = 1) is 2.4×10^{22} Pa s because the lower mantle is set to be 30 times more viscous than the upper mantle. With the temperature contrast of 2000 K across the entire mantle and the present-day potential temperature of 1350 K (Herzberg *et al*., 2007), the temperature contrast across the core-mantle boundary region is 750 K, so with θ of 4.61, the viscosity of ambient lower mantle is $\sim1.3\times10^{23}$ Pa s, which is within the estimated range for the mid-lower mantle viscosity based on instantaneous Stokes flow and postglacial rebound ($\sim2\times10^{22}$ Pa s to $\sim5\times10^{23}$ Pa s) (Forte *et al*., 2015; see their Figure 9) (see also our Figure S-2).

In a similar spirit, other aspects of our convection model are also kept simple; we do not change the temperature contrast across the mantle nor the amount of internal heating. In reality, the temperature contrast should decrease with time because of core cooling. It is not obvious how internal heating would change with time because, as mentioned earlier, internal heating in our model includes both radiogenic heating and secular cooling, so it does not have to monotonically decay with time. Varying the temperature contrast as well as internal heating with time can be done by modeling fully transient mantle convection coupled with the thermal history of the core, but this would inevitably increase the number of poorly constrained model parameters. For example, a hotter mantle in the past does not necessarily mean a less viscous mantle even with a positively temperature-dependent viscosity. Mantle viscosity is also sensitive to the water content (*e.g.*, Karato and Wu, 1993), and the water content of the mantle does not have to be constant with time. In fact, the deep water cycle indicates that the mantle is likely to have been drier in the past (Korenaga *et al*., 2017), which can offset the effect of higher temperature on mantle viscosity (Korenaga, 2011).

Quantifying the Efficiency of Transporting Core Signatures

For 2-D steady-state convection in a closed domain, the streamlines form nested closed loops. The outermost streamline coincides with the domain boundaries, and the parcels that originate at the bottom boundary traverse along all other boundaries. That is, when the base of the bottom boundary layer is brought to the surface by upwelling, it becomes the top of the top boundary layer. A similar situation may be expected for inter-pile convection, and core-affected mantle parcels may be efficiently exposed along the top and side boundaries of the piles. To quantify this, we adopt the following procedure. For each trajectory of entrained dense tracers, we measure its minimum distance to the CMB, and the cumulative distribution of the minimum distance is fitted with the cumulative exponential distribution, $1-\exp(-\lambda z)$, where z is the distance in km and λ is the fitting parameter. Fitting to a cumulative distribution is to make this statistical inference less dependent on model resolution (*e.g.*, the number of tracers involved). For this fitting, we only consider the part of the cumulative distribution that is within the thickness of the bottom boundary layer, which is estimated from the transit time scale as $h \sim 2p\kappa\tau_T/2$. This exponential distribution is compared with the uniform distribution from z =

0 to $z = h$. The slope of the cumulative exponential distribution at $z = 0$ is λ itself, and that of the cumulative uniform distribution is $1/h$. We define the amplification factor as the ratio of these two slopes, *i.e.* λh.

Supplementary Figures

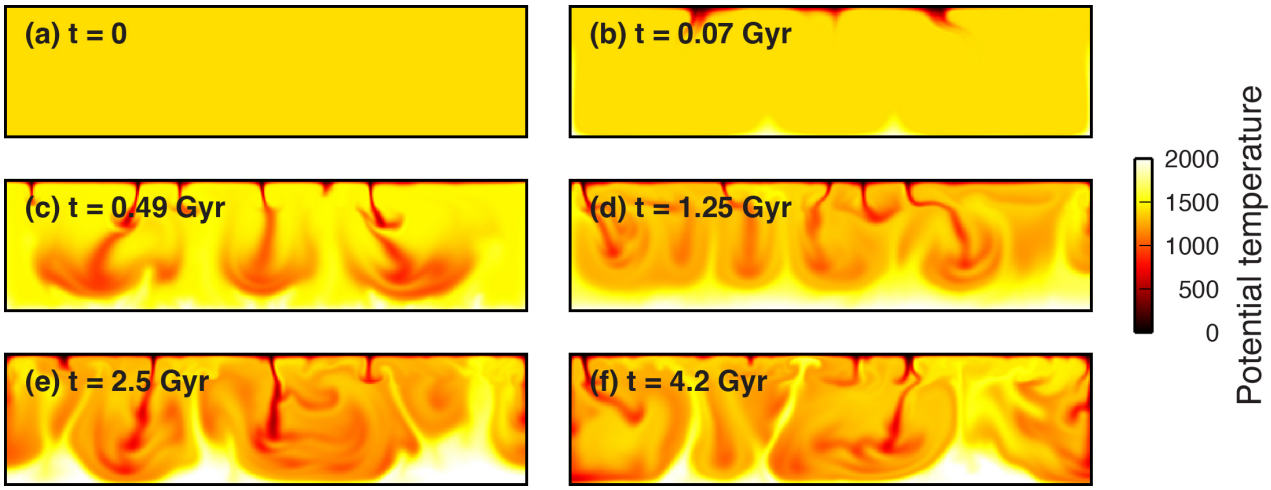

Figure S-1 Snapshots of the temperature field corresponding to those of the composition field shown in Figure 1.

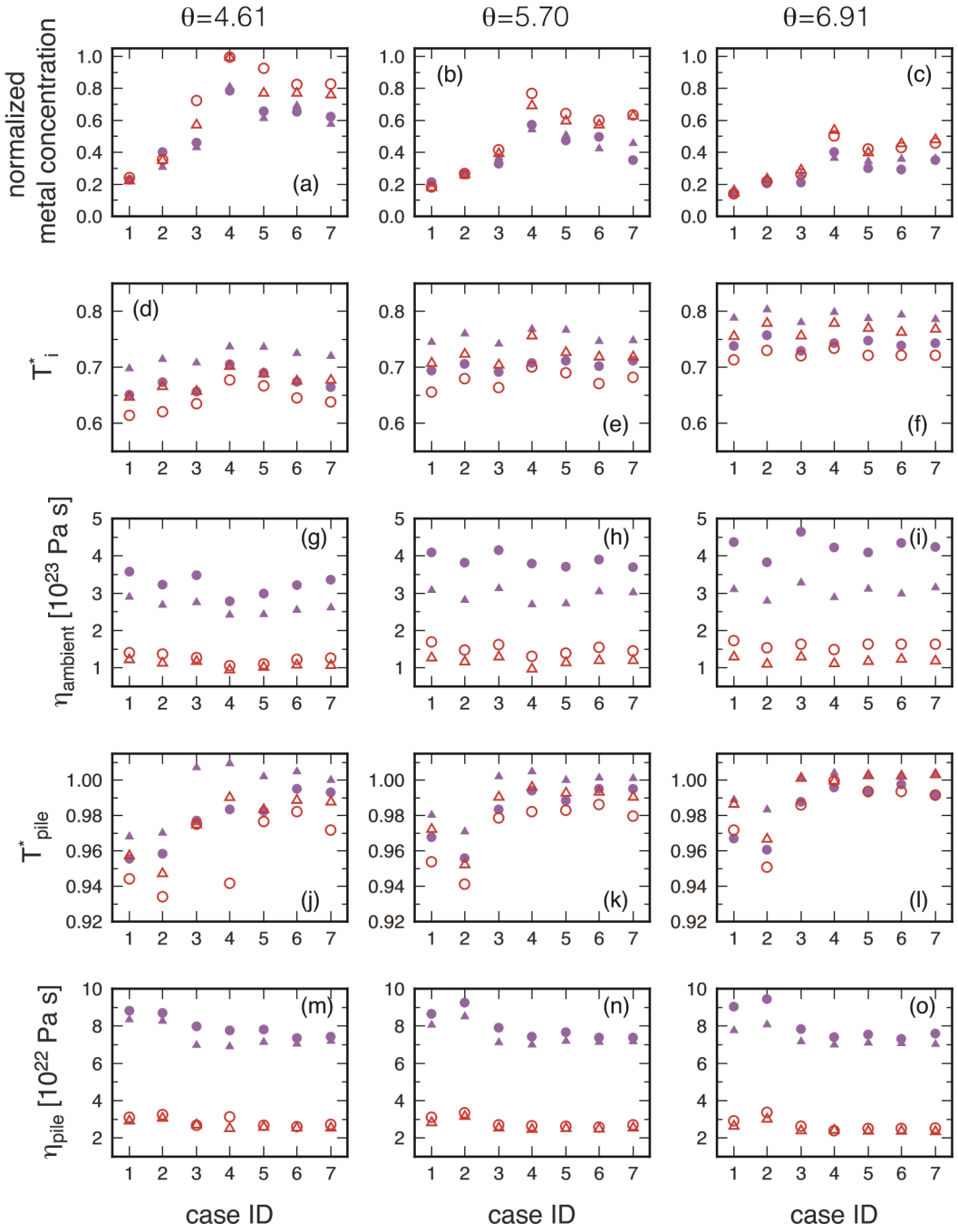

Figure S-2 Diagnostics of convection model runs. The first through the fifth columns show, respectively, normalized metal concentration in the upper mantle (unity corresponding to the observed level) measured at t =4.5 Gyr (present), nondimensional internal temperature, the viscosity of ambient lower mantle, nondimensional pile temperature, and the viscosity of pile. The latter four quantities are time-average from 1 Gyr to 4.5 Gyr. Left, middle, and right columns correspond to different values of the Frank-Kamenetskii parameter as shown. Solid and open symbols are for Ra = 10^7 and 3×10^7, respectively, and circles and triangles denote low and high values for internal heat generation, respectively. See Figure S3 of Korenaga and Marchi (2023) for internal heating ratio and surface heat flux.

Supplementary Information References

Bercovici, D., Tackley, P.J., Ricard, Y. (2015) 7.07 - The Generation of Plate Tectonics from Mantle Dynamics. In: Schubert, G. (Ed.) *Treatise on Geophysics*. Second Edition, Elsevier, Amsterdam, 7, 271–318. https://doi.org/10.1016/B978-0-444-53802-4.00135-4

Christensen, U.R., Yuen, D.A. (1984) The interaction of a subducting lithospheric slab with a chemical or phase boundary. *Journal of Geophysical Research: Solid Earth* 89, 4389–4402. https://doi.org/10.1029/JB089iB06p04389

Forte, A.M., Simmons, N.A., Grand, S.P. (2015) 1.27 - Constraints on Seismic Models from Other Disciplines - Constraints on 3-D Seismic Models from Global Geodynamic Observables: Implications for the Global Mantle Convective Flow. In: Schubert, G. (Ed.) *Treatise on Geophysics*. Second Edition, Elsevier, Amsterdam, 1, 853–907. https://doi.org/10.1016/B978-0-444-53802-4.00028-2

Frazer, W.D., Korenaga, J. (2022) Dynamic topography and the nature of deep thick plumes. *Earth and Planetary Science Letters* 578, 117286. https://doi.org/10.1016/j.epsl.2021.117286

Hager, B.H. (1984) Subducted slabs and the geoid: Constraints on mantle rheology and flow. *Journal of Geophysical Research: Solid Earth* 89, 6003–6015. https://doi.org/10.1029/JB089iB07p06003

Herzberg, C., Asimow, P.D., Arndt, N., Niu, Y., Lesher, C.M., Fitton, J.G., Cheadle, M.J., Saunders, A.D. (2007) Temperatures in ambient mantle and plumes: Constraints from basalts, picrites, and komatiites. *Geochemistry, Geophysics, Geosystems* 8, Q02006. https://doi.org/10.1029/2006GC001390

Karato, S.-I., Wu, P. (1993) Rheology of the Upper Mantle: A Synthesis. *Science* 260, 771–778. https://doi.org/10.1126/science.260.5109.771

Korenaga, J. (2005) Firm mantle plumes and the nature of the core–mantle boundary region. *Earth and Planetary Science Letters* 232, 29–37. https://doi.org/10.1016/j.epsl.2005.01.016

Korenaga, J. (2011) Thermal evolution with a hydrating mantle and the initiation of plate tectonics in the early Earth. *Journal of Geophysical Research: Solid Earth* 116, B12403. https://doi.org/10.1029/2011JB008410

Korenaga, J. (2017) Pitfalls in modeling mantle convection with internal heating. *Journal of Geophysical Research: Solid Earth* 122, 4064–4085, doi:10.1002/2016JB013850. https://doi.org/10.1002/2016JB013850

Korenaga, J., Jordan, T.H. (2003) Physics of multiscale convection in Earth's mantle: Onset of sublithospheric convection. *Journal of Geophysical Research: Solid Earth* 108, 2333. https://doi.org/10.1029/2002JB001760

Korenaga, J., Marchi, S. (2023) Vestiges of impact-driven three-phase mixing in the chemistry and structure of Earth's mantle. *Proceedings of National Academy of Sciences* 120, e2309181120. https://doi.org/10.1073/pnas.2309181120

Korenaga, J., Planavsky, N.J., Evans, D.A.D. (2017) Global water cycle and the coevolution of Earth's interior and surface environment. *Philosophical Transactions of the Royal Society A* 375, 20150393. https://doi.org/10.1098/rsta.2015.0393

Solomatov, V.S. (1996) Can hotter mantle have a larger viscosity? *Geophysical Research Letters* 23, 937–940. https://doi.org/10.1029/96GL00724

Solomatov, V.S. (2001) Grain size-dependent viscosity convection and the thermal evolution of the Earth. *Earth and Planetary Science Letters* 191, 203–212. https://doi.org/10.1016/S0012-821X(01)00426-5